

Digital Simulation of Optimum PWM Inverter Control Asynchronous Motor

A.S.ZEIN EL DIN*, J.F.AUBRY**, S.A.MAHMOUD*

* Electrical Eng. Dept., Faculty of Eng., Shebin El-kom, Menoufia University, Egypt

** CRAN, ENSEM, INPL (CNRS URA 821), Les Nancy, France

Abstract

This paper deals with a digital closed loop speed control of 3-phase induction motor fed by Pulse Width Modulation (PWM) inverter using microprocessor technique. The proposed control relies on a simplified algorithm to compute the optimum switching instants of PWM inverter and the frequency of input voltage to the motor. Starting transients as well as steady state performance of the system including disturbance in load torque, step change in speed reference and step change in torque reference have been studied.

Keywords:

Optimum PWM Inverter, Asynchronous motor, Microprocessor

1. Introduction

Siala and others show that induction motors are widely used in industrial applications due to their attractive price and robustness and consequently, the demand for high-performance control strategies for asynchronous drives is always increases /1/.

The control of electric drives was traditionally carried out by means of analogue devices. It, therefore, benefits of the support of traditional theories of automatic controls. A large technical literature has been made in life. Well-known mathematical methods have been proposed to contribute the theoretical solutions for many practical problems. The production of microprocessor and their

quick development, combined with the continuous reduction of their computing time, make now possible a widespread use of fully digitalized controls for the solution of control problems in electric drives /2/.

Bowes and others indicate that microprocessor control of power-electronic equipment offers the possibility of improvements in manufacture, reliability, maintenance, servicing and increased control flexibility. These advantages inevitably result from a reduction in the complex control circuitry which may be progressively replaced by microprocessor software. It is then possible to change the drive characteristics without altering the hardware. An overview of a possible control hierarchy and distinguishes some of the more desirable features associated with PWM variable speed drive systems /3/.

The speed control of the polyphase induction motor is an art that has attracted a good deal of study in recent years. A number of digital techniques have been developed to utilize their data processing power to control PWM inverter. The natural PWM process, which is based on the analog comparison of a sinusoidal signal and a triangular signal, takes place in real time. This process is believed to be unsuitable for efficient microprocessor implementation, because of the insufficient speed of the presently available microprocessors. As a consequence, various digital methods, such as 'regular-sampled PWM' and 'optimal PWM' techniques, have been developed specifically to suit microprocessor-based implementation /4/.

This paper develops a reasonable digital simulation of PWM inverter control asynchronous motor to check the starting-up and steady state performance of the motor.

2. Optimum Pulse Width Modulation (PWM) inverter model

In microprocessor implemented PWM control schemes /5/, it is very important to develop an efficient and simple model for desired performance.

In the controllers of PWM inverter, it is easy to implement the digital modulation technique. This technique indicates the selection of the switching angles of the inverter output voltage, in such a way that this voltage fulfils given condition. Among the digital techniques, the harmonic technique and that of the optimum waveform

are the most common, a typical voltage waveform of the input PWM voltage inverter is shown in Fig.1, it exhibits quarter wave and half-wave symmetry (M=3), the switching pattern α satisfies the following relations :

$$0 < \alpha_1 < \alpha_2 < \alpha_3 \text{ --- } \alpha_M < \pi/4 \text{ ---} \quad (1)$$

The r -th harmonics of the waveform of Fig.1, is equal to :

$$V_r = \frac{4E}{\pi r} \left(1 - 2 \sum_{i=1}^{M+1} (-1)^{i+1} \cos(r \alpha_i) \right) \text{ ---} \quad (2)$$

The constraints imposed on α by the harmonic elimination technique, for each r th harmonics to be eliminated are :

$$r \neq 1, \quad V_r(\alpha) = 0 \text{ ---} \quad (3)$$

$$V_1 = \frac{4E}{\pi} \left(1 - 2 \sum_{i=1}^{M+1} (-1)^{i+1} \cos(\alpha_i) \right) \text{ ---} \quad (4)$$

The solution of the non linear equations 1 \longrightarrow 4 requires very complex numerical algorithms. The pulse-widths or switching angles for some levels of the first harmonics of the inverter output voltage can be obtained in off time and stored in the microprocessor memory as a look-up table, the task of obtaining the angles, allows it to operate in real time /6/. The microprocessor acts simply as a pulse generator producing pulses of predetermined widths. With PWM techniques, one look-up table corresponds to a certain magnitude of the inverter output voltage. If the output voltage is to be varied, it becomes necessary to prepare a number of look-up tables each corresponding to a certain output voltage level. The microprocessor is then programmed to switch from one look-up to another in order to change the output voltage magnitude for keeping $V/F = \text{constant}$.

3. The d-q representation of 3-phase induction motor

A 3-phase induction motor supplied by PWM inverter is considered. Neglecting its core losses, saturation effects and space harmonics, the motor can be described by the following set of equations:

$$\Psi_{ds} = L_s i_{ds} + L_{sr} i_{dr} \quad (5) \quad \Psi_{qs} = L_s i_{qs} + L_{sr} i_{qr} \quad (6)$$

$$\Psi_{dr} = L_r i_{ds} + L_{sr} i_{ds} \quad (7) \quad \Psi_{qr} = L_r i_{qs} + L_{sr} i_{qs} \quad (8)$$

$$d\Psi_{ds}/dt = V_{ds} + W_a \Psi_{qs} - R_s i_{ds} \quad (9)$$

$$d\Psi_{qs}/dt = V_{qs} - W_a \Psi_{ds} - R_s i_{qs} \quad (10)$$

$$d\Psi_{dr}/dt = V_{dr} + (W_a - W_R) \Psi_{qs} - R_r i_{dr} \quad (11)$$

$$d\Psi_{qr}/dt = V_{qr} - (W_a - W_R) \Psi_{ds} - R_r i_{qr} \quad (12)$$

$$V_{ds} = 2/3 [V_a \cos \theta + V_b \cos(\theta - \frac{2\pi}{3}) + V_c \cos(\theta + \frac{2\pi}{3})] \quad (13)$$

$$V_{qs} = 2/3 [V_a \sin \theta + V_b \sin(\theta - \frac{2\pi}{3}) + V_c \sin(\theta + \frac{2\pi}{3})] \quad (14)$$

$$V_{dr} = V_{qr} = 0 \quad (15) \quad S = (W_e - P W_m) / W_e \quad (16)$$

$$T_e = 3/2 P L_{sr} [i_{qs} i_{dr} - i_{ds} i_{qr}] = T_f + K W_m + J dW_m/dt \quad (17)$$

$$W_e = 2 \pi F \quad (18) \quad W_R = P W_m \quad (19)$$

$$i_{ds} = 2/3 [i_a \cos \theta + i_b \cos(\theta - \frac{2\pi}{3}) + i_c \cos(\theta + \frac{2\pi}{3})] \quad (20)$$

$$i_{qs} = 2/3 [i_a \sin \theta + i_b \sin(\theta - \frac{2\pi}{3}) + i_c \sin(\theta + \frac{2\pi}{3})] \quad (21)$$

From eqs. (20) & (21) at $\theta = 0$ $i_{ds} = i_a$ and at $\theta = 90^\circ$ $i_{qs} = i_a$

From eqs. (5) \rightarrow (8), the following simplified Eqs. are

$$i_{ds} = [L_{sr} \Psi_{dr} - L_r \Psi_{ds}] / [L_{sr}^2 - L_s L_r] \quad (22)$$

$$i_{qs} = [L_{sr} \Psi_{qr} - L_r \Psi_{qs}] / [L_{sr}^2 - L_s L_r] \quad (23)$$

$$i_{dr} = [\Psi_{ds} - L_s i_{ds}] / [L_{sr}] \quad (24)$$

$$i_{qr} = [\Psi_{qs} - L_s i_{qs}] / [L_{sr}] \quad (25)$$

171

The equations 9 \rightarrow 25 are solved numerically using the Runge Kutta method, with a sufficiently small step length.

4. Basic structure of the control system

A closed-loop system generally has the advantages of greater accuracy, improved dynamic performance and reduced effect of disturbances such as loading. When the drive requirements include rapid acceleration and deceleration, closed-loop control is necessary. The basic block diagram of the control system is shown in Fig. 2, the feedback

angular speed of the motor (W_m) is compared with the reference angular speed W_{ref} and the difference ΔW_m is modified by PI controller algorithm of speed to obtain ΔW which added to W_m to obtain Δe and multiplied by factor $P/2\pi$ to obtain Δe_1 . The equation of each part of the system is developed as follows :

$$\Delta W_m(t) = K_s W_m(t) + K_s/T_s \int_0^t W_m(t) dt \quad \text{-----} \quad (26)$$

$$\Delta W_m(t) = W_{ref} - W_m(t) \quad \text{-----} \quad (27)$$

$$\Delta e(t) = W_m(t) + W_m(t) \quad \text{-----} \quad (28)$$

$$\Delta e_1(t) = P \Delta e / 2\pi \quad \text{-----} \quad (29)$$

The rotor speed (W_m), d-c link voltage, stator phase currents and flux can be measured. The electromagnetic torque of the motor is computed from equation (17), and compared with the reference torque (T_{ref}), the difference between them ΔT is modified by the PI controller algorithm to obtain $\Delta e_2(t)$ which added to $\Delta e_1(t)$ to obtain the required frequency of PWM inverter. Using a suitable algorithm to select the required look-up table, contains the switching points of optimum PWM inverter (or the required angles α_i), d-c link input voltage of the inverter can be controlled to keep $E/F = \text{constant}$.

$$F <= F_n \ \& \ E = V_n \ \text{if } F > F_n \quad \text{-----} \quad (30)$$

The PI controller of torque can be achieved by the following Equations :

$$\Delta e_2(t) = K_T T(t) + K_T/T_r \int_0^t W_m(t) dt \quad \text{-----} \quad (31)$$

$$\Delta T(t) = T_{ref} - T_e(t) \quad \text{-----} \quad (32)$$

5. Simulation Results

The simulations have been carried out on the motor with the following parameters :
 full load torque=9.25n.m., rated speed=1418r.p.m.,
 $V_n = 310.3$ volt., $J = 0.009$ kg.m², $L_r = 0.34$ h, $L_s = 0.34$ h,
 $L_{sr} = 0.318$ h, $R_s = 4.7$ ohm, $R_r = 4.1$ ohm, $P = 2$ and for the PI controllers of speed and torque, the

parameters are: $K_s=10$, $T_s=0.0001$, $K_r=10$, $T_r=0.0001$, $N_{ref}=1410$ r.p.m., $W_{ref} = 2\pi N_{ref}/60$., $T_{ref}=9.5$ n.m., and for the optimum PWM inverter voltage : no of harmonics elimination=50, $V_r(\alpha_i)=0$, $r < 1$, $M=3$, $\alpha_1=0.0785$ rad., $\alpha_2=0.196$ rad., $\alpha_3=0.2748$ rad. The input of the actual motor speed was performed continuously through encoder circuit connect to the microprocessor. The stator phase currents of the motor were connected to microprocessor through A/D circuit.

5.1 Motor starting without controller

Starting-up transient of loaded motor fed by 3-phase optimum PWM inverter has been considered. Fig.3 shows the performance of the motor during transient and steady state periods. The minimum and maximum values of the currents, flux, speed, torque and frequency are as given in Table 1.

	min. and max. i_{ds} (amp.)	min. and max. i_{qs} (amp.)	min. and max. torq. (n.m.)	min. and max. i_{dr} (amp.)	min. and max. i_{qr} (amp.)	min. and max. Ψ_{ds} (wb.)	min. and max. Ψ_{qs} (wb.)	min. and max. Ψ_{dr} (wb.)	min. and max. Ψ_{qr} (wb.)	min. and max. N_r (r.p.m.)	min. and max. freq. (hz.)
trans	-28.66	-23.3	-3.24	-21.12	-23.5	-1.62	-1.26	-1.083	-1.052	0	50
trans	21.26	24.28	52.05	25.55	22.04	1.68	1.136	1.083	1.053	1469.4	50
s.s.	-4.46	-4.596	8.123	-3.055	-2.814	-1.159	-1.115	-1.081	-1.052	1447.6	50
s.s.	4.462	4.596	10.31	3.055	2.813	1.159	1.115	1.081	1.051	1448.8	50

Table 1 Performance of the motor during transient and steady state periods (without controller)

5.2 Motor starting with controller

A desirable approach for control systems is to incorporate all digital control loop. There are many advantages of this approach. The digital control loop eliminates the need for traditional analog compensation circuits and their associated multiplicity of adjustments.

The parameters of closed-loop speed and torque control are: ($K_s=10$ & $T_s=0.0001$), $T_{ref}=9.5$ n.m.,

$N_{ref}=1410$ r.p.m., $W_{ref} = 2\pi \frac{N_{ref}}{60}$, $K_r=10$ and $T_r=0.0001$.

Fig.4 shows the performance of the motor during the transient and the steady state periods. The minimum and maximum values of the currents, flux, torque, speed and frequency are given in Table 2.

	min. and max. i_{ds} (amp.)	min. and max. i_{qs} (amp.)	min. and max. torque (n.m.)	min. and max. i_{dr} (amp.)	min. and max. i_{qr} (amp.)	min. and max. Ψ_{ds} (wb.)	min. and max. Ψ_{qs} (wb.)	min. and max. Ψ_{dr} (wb.)	min. and max. Ψ_{qr} (wb.)	min. and max. N_r (r.p.m.)	min. and max. freq. (hz.)
trans	-28.66	-23.46	-8.25	20.68	-24.07	-1.62	-1.314	-0.934	-0.917	0	32.6
trans	20.62	25	49.3	25.55	22.07	1.092	1	0.932	0.919	1430.3	567.5
s.s.	-4.558	-4.061	8.976	-3.031	-3.238	-0.994	-0.959	-0.924	-0.909	1429.1	41
s.s.	4.05	4.606	9.538	3.226	3.227	0.998	0.963	0.927	0.912	1429.5	46.7

Table 2 Performance of the motor during transient and steady state periods (with controller) $T_{ref} = 9.5$ n.m. and $N_{ref} = 1410$ r.p.m.

5.3 Load torque disturbance

The performance of the motor is shown in Fig.5, the load torque is stepped down from its full load torque value to 0.8 full load. The minimum and maximum values of the currents, flux, torque, speed and frequency are given in Table 3.

	min. and max. i_{ds} (amp.)	min. and max. i_{qs} (amp.)	min. and max. torque (n.m.)	min. and max. i_{dr} (amp.)	min. and max. i_{qr} (amp.)	min. and max. Ψ_{ds} (wb.)	min. and max. Ψ_{qs} (wb.)	min. and max. Ψ_{dr} (wb.)	min. and max. Ψ_{qr} (wb.)	min. and max. N_r (r.p.m.)	min. and max. freq. (hz.)
trans.	-5.08	-5.145	4.935	-3.115	-3.264	-1.18	-1.188	-1.089	-1.088	1425.6	41.2
trans.	5.464	5.196	9.47	-3.27	3.027	1.174	1.194	1.089	1.09	1465	81.2
s.s.	-4.288	-4.13	6.087	-2.373	-2.464	-1.16	-1.166	-1.089	-1.088	1449.7	47.7
s.s.	4.639	4.471	8.248	2.379	2.243	1.172	1.181	1.083	1.084	1457.1	73.2

Table 3 Performance of the motor during transient and steady state periods (with controller), $T_{ref} = 9.5$ n.m. and $N_{ref} = 1410$ r.p.m., load torque is stepped down by 20% of full load torque

5.4 Load torque disturbance and step change in torque reference

Figure 6 shows the performance of the motor if the load torque is suddenly stepped down by 20% from its full load value and also the torque reference is stepped down from 9.5 n.m. to 7.6 n.m. The minimum and maximum values of the currents, flux, torque, speed and frequency are given in Table 4.

	min. and max. i_{ds} (amp.)	min. and max. i_{qs} (amp.)	min. and max. torque (n.m.)	min. and max. i_{dr} (amp.)	min. and max. i_{qr} (amp.)	min. and max. Ψ_{ds} (wb.)	min. and max. Ψ_{qs} (wb.)	min. and max. Ψ_{dr} (wb.)	min. and max. Ψ_{qr} (wb.)	min. and max. N_r (r.p.m.)	min. and max. freq. (hz.)
tran	-4.722	-4.61	6.928	-3.25	-3.302	0.991	-1.04	-0.911	-0.907	1425.6	35.55
tran	4.828	4.617	9.018	3.28	3.227	1.016	0.99	0.931	0.926	1439	47.4
s.s.	-3.934	-3.961	7.186	-2.926	-2.763	-0.35	-0.938	-0.879	-0.874	1435.6	37.98
s.s.	3.943	3.981	7.703	2.874	2.738	0.898	0.948	0.888	0.874	1436.5	43.62

Table 4 Performance of the motor during transient and steady state periods (with controller), T_{ref} is stepped down from 9.5 n.m. to 7.4 n.m., $N_{ref} = 1410$ r.p.m. and load torque is stepped down by 20% full load torque .

5.5 step change in speed reference

Figure 7 shows the performance of the motor when the stepped down the speed reference by 20% (from $N_{ref}=1410$ r.p.m. to $N_{ref}=1126$ r.p.m.) at the torque reference = 9.5 n.m. Table 5 shows the minimum and maximum values of currents, flux, torque, speed and frequency during the steady state and transient periods.

	min. and max. I_{ds} (amp.)	min. and max. I_{qs} (amp.)	min. and max. T_{qr} (n.m.)	min. and max. I_{dr} (amp.)	min. and max. I_{qr} (amp.)	min. and max. Ψ_{ds} (wb.)	min. and max. Ψ_{qs} (wb.)	min. and max. Ψ_{dr} (wb.)	min. and max. Ψ_{qr} (wb.)	min. and max. N_r (r.p.m.)	min. and max. freq. (hz.)
trans	-7.648	-7.893	0.831	-7.116	-7.212	-0.657	-0.607	-0.809	-0.695	1170.6	19.41
trans	7.66	7.885	9.364	7.117	7.222	1.016	0.835	0.931	0.895	1425.6	47.4
s.s.	-7.646	-7.877	9.07	-7.11	-7.21	-0.552	-0.557	-0.425	-0.425	1170.6	25.42
s.s.	-7.65	7.885	9.384	7.104	7.2	0.55	0.558	0.424	0.425	1171.2	28.31

Table 5 Performance of the motor during transient and steady state periods (with controller), N_{ref} is stepped down from 1410 r.p.m. to 1126 r.p.m. and $T_{ref} = 9.5$ n.m.

5.6 Step change in torque reference

The performance of the motor is shown in Fig.8 when the torque reference is stepped up from 9.5 to 11.4 n.m. at speed reference = 1410 r.p.m. Table 6 shows the minimum and maximum values of currents, flux, torque, speed and frequency during the steady state and transient periods.

	min. and max. I_{ds} (amp.)	min. and max. I_{qs} (amp.)	min. and max. T_{qr} (n.m.)	min. and max. I_{dr} (amp.)	min. and max. I_{qr} (amp.)	min. and max. Ψ_{ds} (wb.)	min. and max. Ψ_{qs} (wb.)	min. and max. Ψ_{dr} (wb.)	min. and max. Ψ_{qr} (wb.)	min. and max. N_r (r.p.m.)	min. and max. freq. (hz.)
trans	-5.633	-5.549	7.131	-3.592	-3.765	-1.172	-1.176	-1.077	-1.079	1425.6	42.54
trans	5.687	5.53	11.31	3.835	3.709	1.161	1.166	1.081	1.08	1452.7	80.84
s.s.	-4.47	-4.63	8.4	-3.099	-2.93	-1.137	-1.147	-1.064	-1.063	1445.4	46.92
s.s.	4.55	4.579	10.28	3.129	2.999	1.14	1.145	1.07	1.087	1449.8	65.60

Table 6 Performance of the during transient and steady state periods (with controller), T_{ref} is stepped up from 9.5 n.m. to 11.4 n.m. and $N_{ref}=1410$ r.p.m.

Also, by controlling the reference speed or the reference torque, it is possible to control the performance of the motor. It can be noted that from the comparison between the starting-up of the motor without controller and with controller, the possibility to control the over shoot of the speed by controlling ω_{ref} ($\omega_{ref} = 2\pi N_{ref}$), the fluctuating of speed during the steady state period and without using the controller is between 1447.6 and 1448.817 r.p.m. and it is between 1429.135 and

1429.54 r.p.m. with the controller and $N_{ref} = 1410$ r.p.m. Also the fluctuating of torque during steady state period is between 8.123 and 10.31 n.m. without using controller and it is between 8.976 and 9.538 n.m. with using the controller and $T_{ref} = 9.5$ n.m. If the disturbance in load torque has occurred, the performance of the motor is still with the acceptable limits.

6. Conclusions

A proposed simplified algorithm has been provided. Performance of the motor during starting-up and steady-state periods have been studied. The results showed that the motor speed due to the disturbance in load torque is still with the acceptable limit.

7. Reference

- 1- Sami Siala, Bernard de Fornel, Maria Pietrzak, "Comparison study of continuous and sampled control performances in asynchronous drives", IMACS-TC1'90 Nancy, 19-20-21, France, 1990.
- 2-C.Attaianesi, G.Manco, E.Pagano, "Philosophy of use of microprocessors for digital control of asynchronous motors", IEEE Industrial Electronics Society Proceedings MCECD'1991, Marseille, 1-2 July 1991.
- 3-S.R.Bowes, C.Eng., M.I.Mech., M.I.E.E. and M.J.Mount, "Microprocessor control of PWM inverter", IEE Proc., vol.128, I.B., no.6, 1981.
- 4-E.S.Tez, "Motonic chip set: high performance intelligent controller for industrial variable speed a.c. drives", IEEE conference publication no.291, 1981.
- 5-C.C.Chan, K.T.Chau, "A new PWM algorithm for battery source three phase inverters", Electric Machines and power systems 19:43-54., 1991.
- 6-Giuseppe S.Buja and Paolo Fiorini, "Microprocessor control of PWM inverter", IEEE trans. on Industrial electronic, vol. IE-29, no.3, 1982.
- 7-Asish.K.De Sarkar and Gunnar.J.Berg., "Digital simulation of three-phase induction motors", IEEE Trans. on power apparatus and system, vol.pas-89, no.6, 1970.
- 8-T.Green and B.W.Williams, "A gate array design for PWM inverter control", EPE Aachen, 1989.
- 9-M.J.Case, K.C.Burgers, "A controller for rapid induction motor torques step responses", EPE Aachen, 1989.

10-A.S.Zein El Din, A.E.Azzam, A.A.El Hefnawy,
 "Simulation of microprocessor closed loop control
 of induction motor fed by optimum PWM inverter
 drive", Amse press., vol.2 pp.77-96, Marok, 1990.

List of symbols

Ψ_{ds}, Ψ_{qs} : direct and quadrature axes stator flux linkage
 Ψ_{dr}, Ψ_{qr} : direct and quadrature axes rotor flux linkage
 α_i : i th switching angle ($i = 1 \dots M$)
 E : Maximum value of output voltage of PWM inverter.
 F : frequency of input voltage of the motor
 F_n : nominal frequency of the input voltage
 I_{ds}, I_{qs} : direct and quadrature axes components of stator current.
 I_{dr}, I_{qr} : direct and quadrature axes components of rotor current.
 i_a, i_b, i_c : currents of phases a, b and c resp.
 J, K : moment of inertia and friction constant
 K_s, K_r : proportional gain constant of speed and torque PI controller
 L_s, L_r : apparent three phase stator and rotor self-inductance
 L_{sr} : apparent three phase mutual-inductance
 M : no of switching angles per quarter cycle
 N_{ref} : reference rotor speed in r.p.m.
 P : no of pair poles
 R_s, R_r : stator and rotor resistance
 S : slip of the motor = $(\omega_e - \omega_r) / \omega_e$
 θ : arbitrary electrical angular position
 t : time in sec.
 T_e : electromagnetic torque
 T_{ref} : reference torque
 T_s, T_r : time constant of speed and torque PI controller
 T_L : load torque
 V_a, V_b, V_c : voltage of phases a, b and c
 V_{ds}, V_{qs} : direct-and-quadrature axes component of stator voltage
 V_{dr}, V_{qr} : direct-and-quadrature axes component of rotor voltage
 V_r : r th harmonic of the input voltage wave form of PWM inverter
 V_n : nominal amplitude of the motor input voltage
 ω_a : arbitrary electrical angular velocity
 ω_e : electrical angular velocity = $2 \pi F$
 ω_m : rotor angular velocity
 ω_{ref} : reference angular velocity = $2 \pi N_{ref} / 60$
 ω_R : electrical angular rotor speed

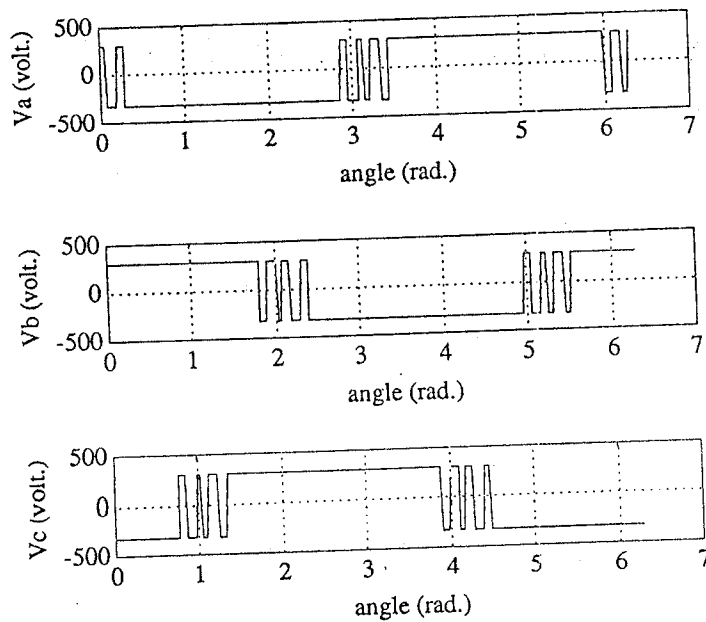


Fig.(1) optimum PWM inverter voltage in phase a, phase b and phase c

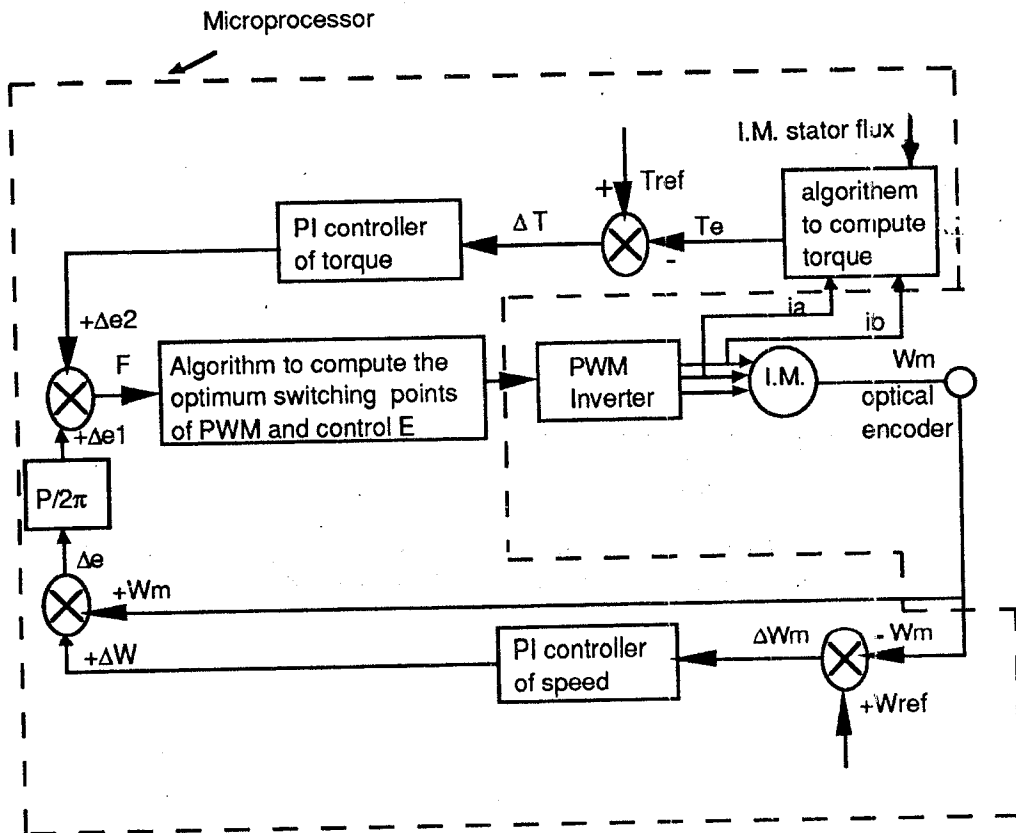


Fig.(2) Basic schematic diagram of the control system

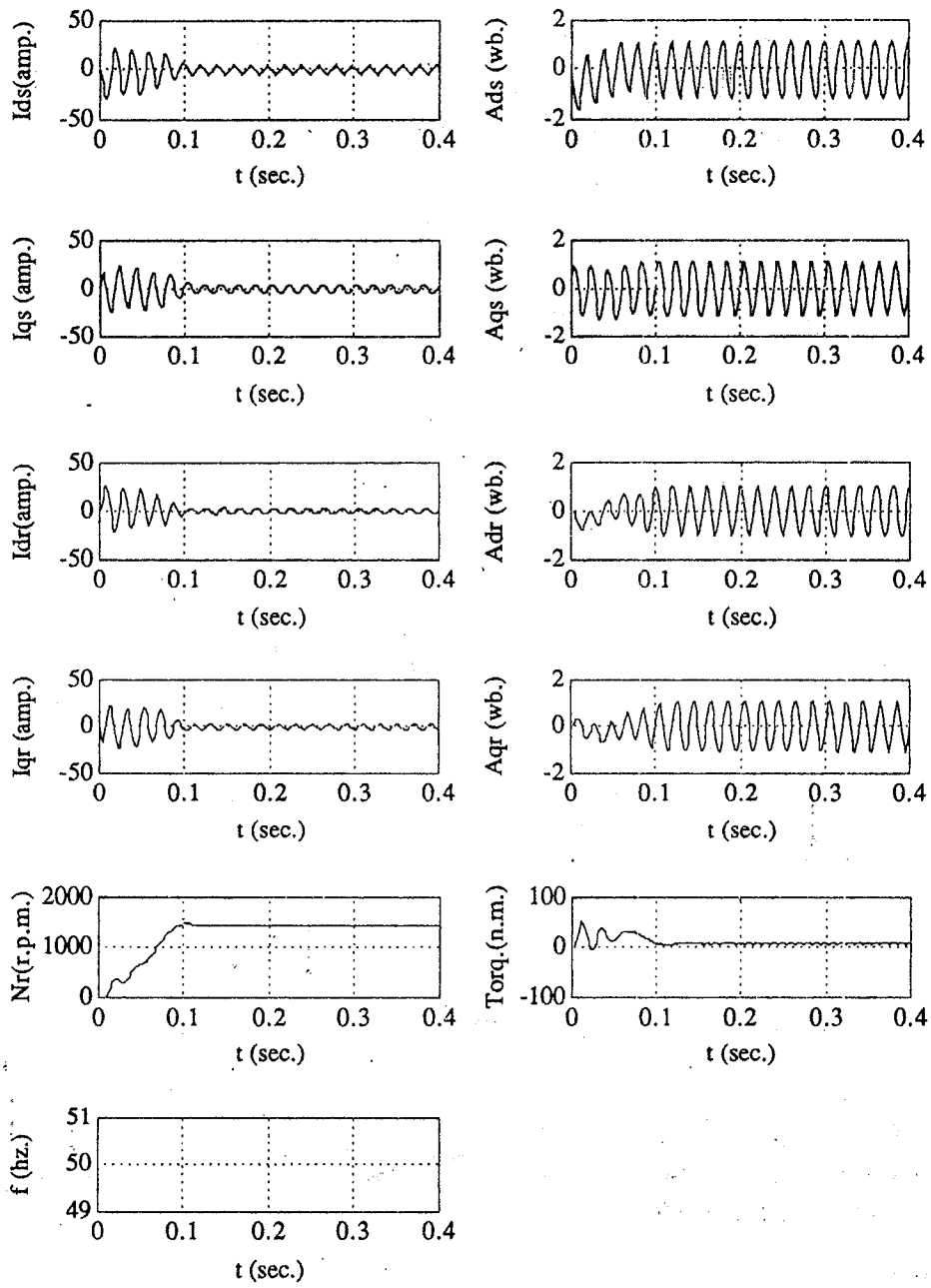


Fig.(3) The performance of the motor during starting period and steady state period without controller and fed by optimum PWM inverter

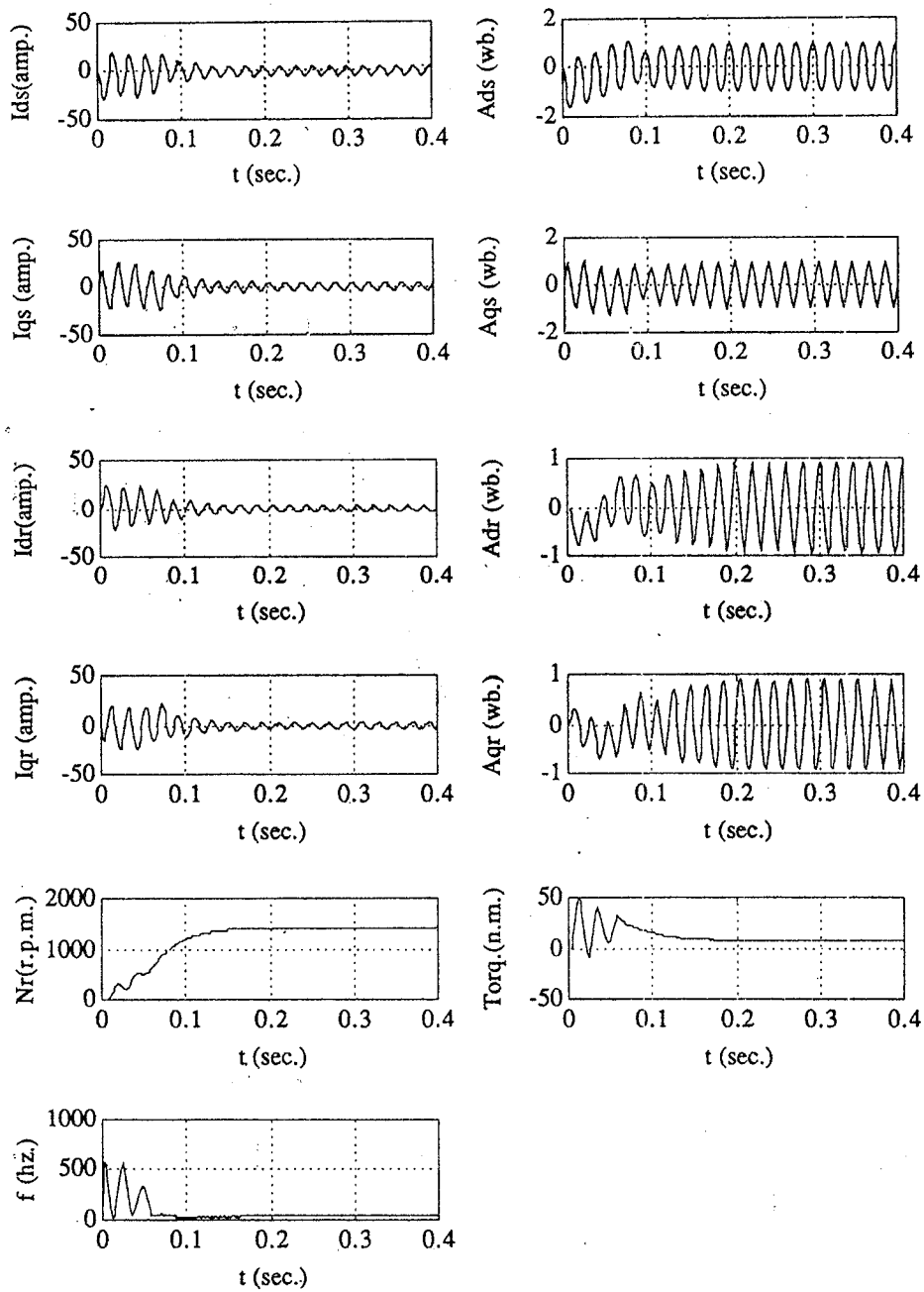


Fig.(4) The performance of the motor during starting period and steady state period with controller and fed by optimum PWM inverter ($T_{ref}=9.5$ n.m. & $N_{ref} = 1410$ r.p.m.)

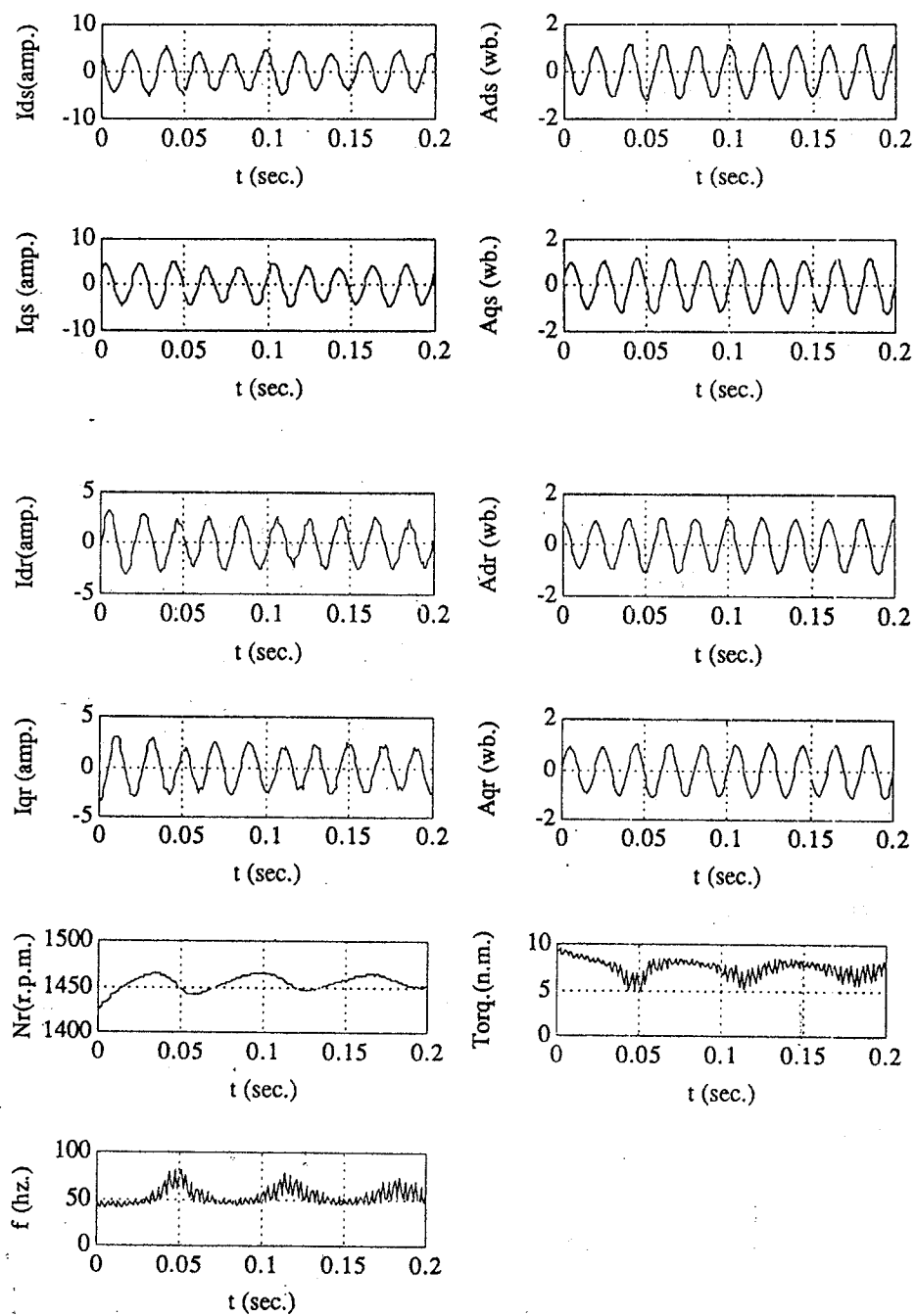


Fig.(5) The performance of the motor during step down of load torque by 20% full load torque and $T_{ref} = 9.5$ n.m. & $N_{ref} = 1410$ r.p.m.

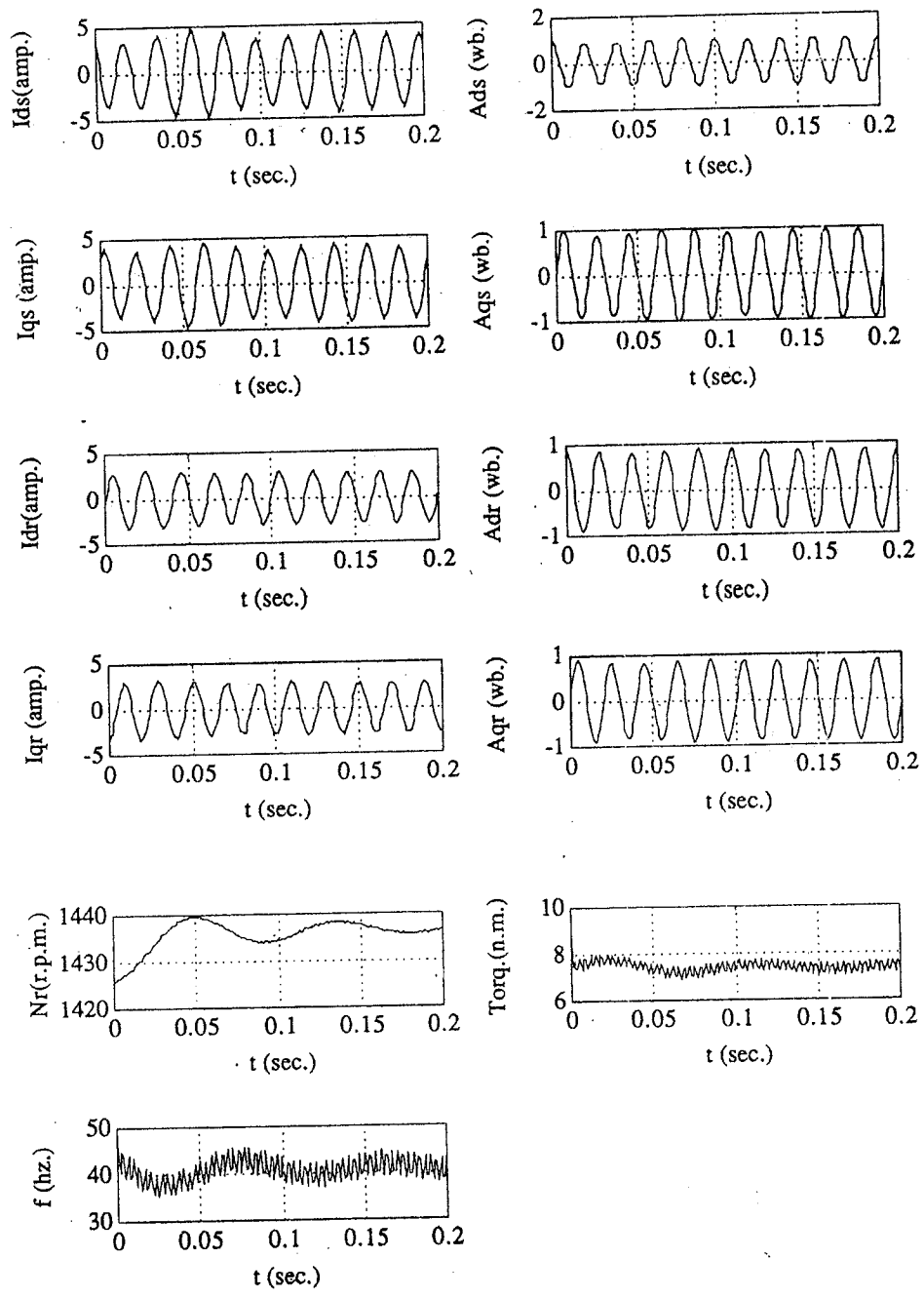


Fig.(6) The performance of the motor during step down of load torque by 20% full load torque and T_{ref} is stepped down from 9.5 n.m. ----> 7.4 n.m. & $N_{ref} = 1410$ r.p.m.

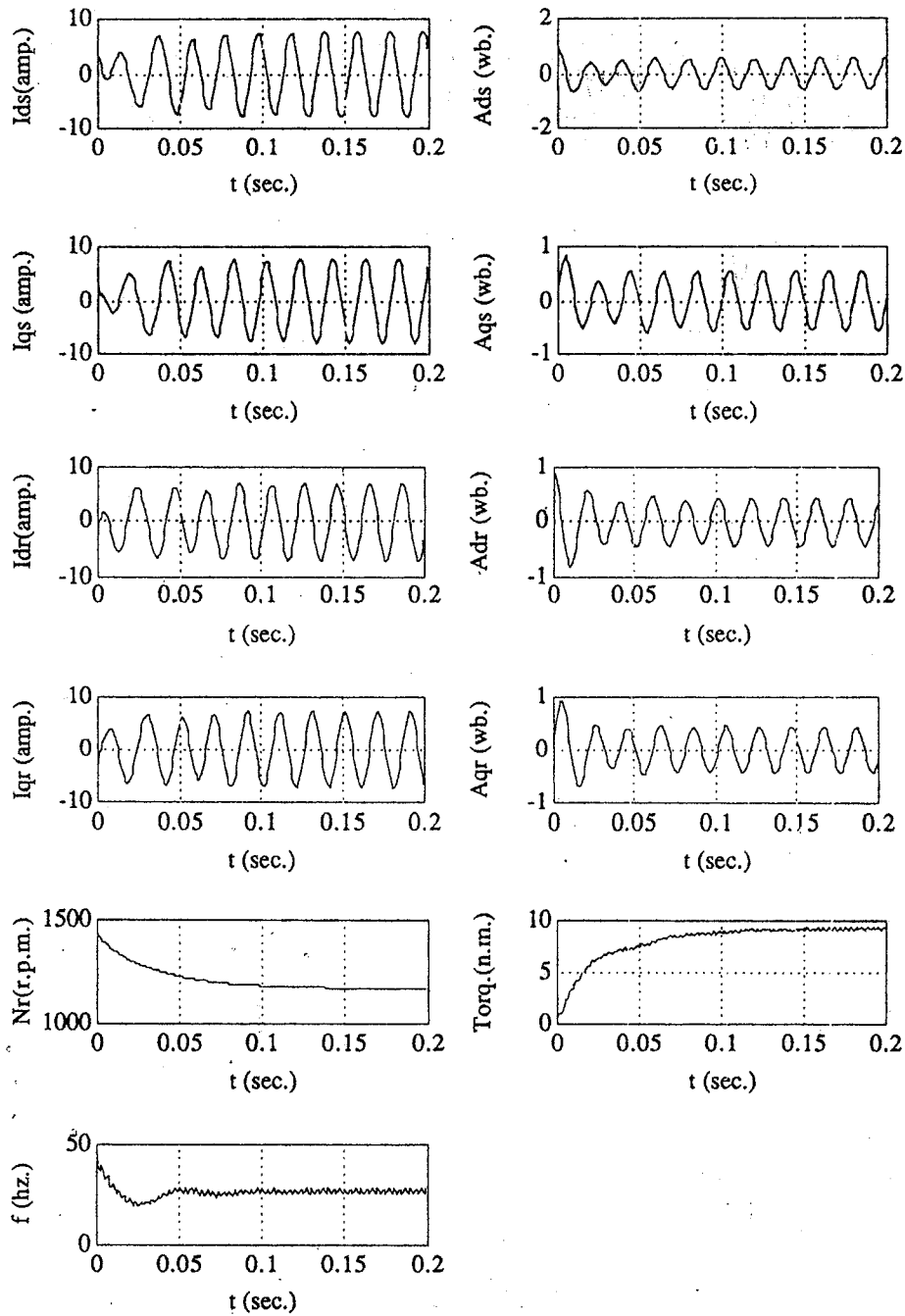


Fig.(7) The performance of the motor during step down of N_{ref} by 20% rated value ($T_{ref}=9.5$ n.m. & $N_{ref} = 1410$ r.p.m. -----> 1126 r.p.m.)

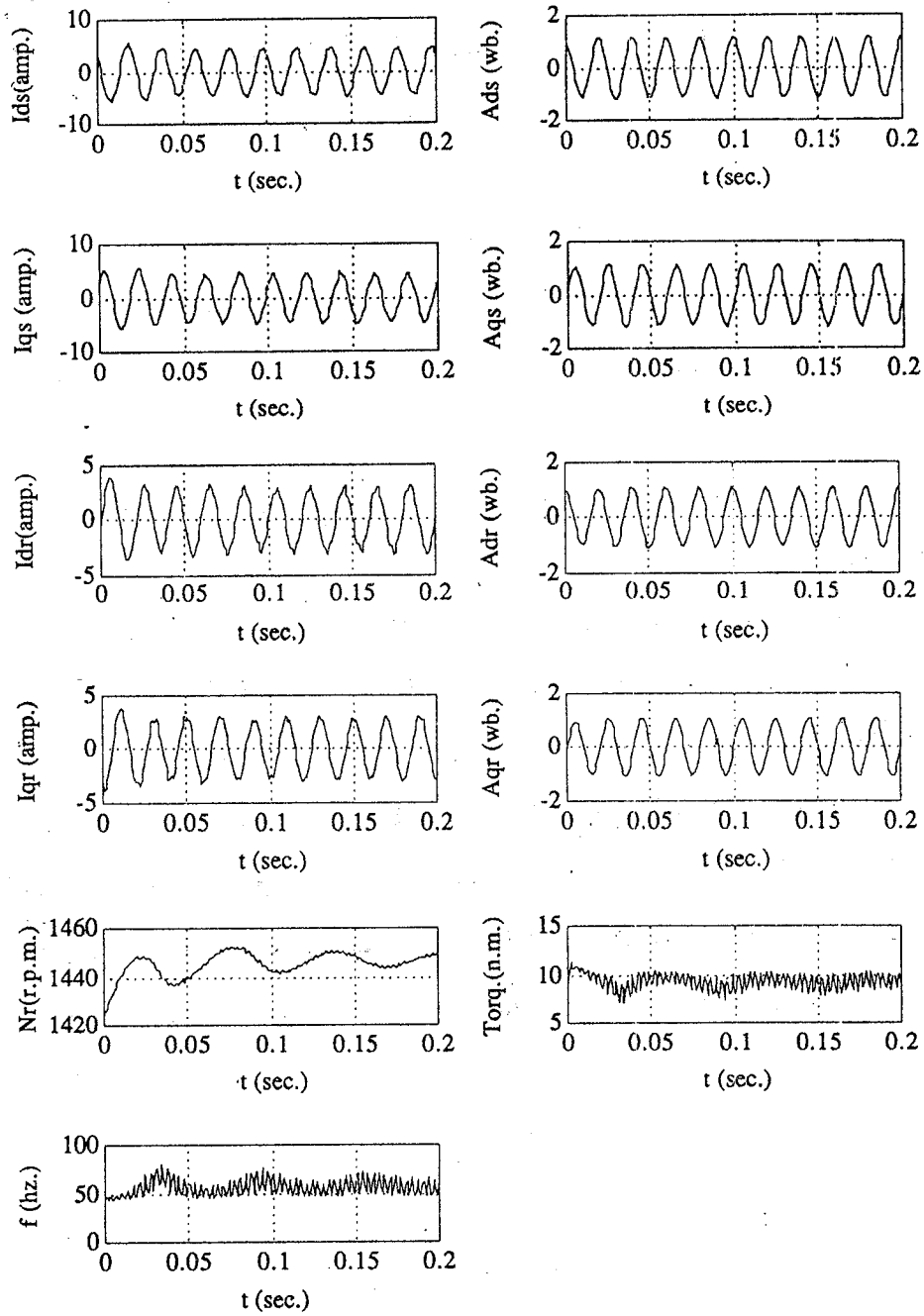


Fig.(8) The performance of the motor during step up of T_{ref} by 20% rated value ($T_{ref} = 9.5$ n.m. \rightarrow 11.4 n.m. & $N_{ref} = 1410$ r.p.m.)

التحكم الرقمي في سرعة محرك حثي ثلاثي الوجه باستخدام التعديل النبضي الأمتل للحصول على تيار متغير

المخلص

في الآونة الأخيرة ظهرت تطبيقات عديدة باستخدام أساليب الميكروبروسيسور في مجال التحكم في المحركات ذات السرعات المتغيرة مثل المحرك الحثي ثلاثي الأوجه . ويتناول هذا البحث طريقة مبتكرة للتحكم المحكم في سرعة محرك حثي ثلاثي الأوجه المغذى بجهد متغير التردد وذلك باستخدام الميكروبروسيسور . الطريقة المقترحة في التحكم تعتمد على أساس بناء الخوريزم مبسط يقوم بحساب لحظات التوصيل لمقطع الجهد باستخدام التعديل النبضي الأمتل للحصول على تيار متغير يحتوى على أقل عدد ممكن من التوافقيات وبالتالي التحكم في تردد الجهد المتغير المغذى للمحرك تحت شرط ثبوت الفولت/التردد أثناء التشغيل . وتشتمل البحث على دراسة لأداء المحرك خلال الفترات الإنتقالية والإستقرار عند حدوث تغير مفاجئ في الحمل و أيضا عند حدوث تغير في محدد قياس السرعة المقارن .